Evaluating the Impact of Nutrient Management on Groundwater Quality in the Presence of Deep Unsaturated Alluvial Sediment

FREP Contract # 01-0584

Project Leader
Thomas Harter, Ph.D.
Assoc. Coop. Ext. Specialist
Department of Land, Air and Water Resources
University of California
Davis, CA 95616

UC Davis Project Collaborators:
Timothy Ginn, Ph.D. Department of Civil Engineering

Jan Hopmans, Ph.D. Department of Land, Air and Water Resources

William Horwath, Ph.D. Department of Land, Air, and Water Resources

Introduction

As part of an overall study of the role of the alluvial unsaturated zone in controlling the long term impact of California Central Valley agricultural practices on groundwater quality, we here report on completed tasks in Subtask 1 under Year1: Task 1 in the work plan. This interim report includes the period of April 2002-September 2002 as stated in the work plan. The accomplished tasks include: 1) data management and interpretation including soil hydraulic properties, and biochemical characterization of the deep unsaturated zone, irrigation, fertilizer and climate data at the research site, 2) implementation of geostatistical analysis of the dataset, and 3) quantitative analysis of the subsurface nitrate budget in the vadose zone. The last task is done using different methods.

1. Data Construction and Interpretation

The first phase of the study includes gathering detailed description of soil hydraulic properties and biochemical characterization of the deep unsaturated zone at the Kearney Research Site located in the Eastern San Joaquin Valley, 20 km southeast of Fresno on the Kings River alluvial fan. Elevation of the site is 103 m (~337 ft) above the sea level, and annual rainfall is about 270 mm, occurring mainly during winter months. The experimental site is a former orchard of Fantasia nectarine at the University of California Kearney Agricultural Center. The orchard was subject to a 12-year fertilizer management experiment (from 1982 to 1995) involving a plot of 15 rows with 15 trees per row with a distance of 20 ft (~6.1 m) between trees in both N-S and E-W directions. The orchard was divided into 14 subplots, each consists of five trees in a row (see Figure 1). During the fertilizer experiment, five treatments with 0, 100, 175, 250, and 325 lbs/acre/year application rate were applied to the 14 subplots, each consisting of five trees in a row. 100, 175, 250, 325 lbs/acre/year treatments had 3 replicas while 0 lbs/acre treatment had only two replicas. During 1997-98, upon completion of the fertilizer experiment, three

subplots, fertilized at the annual rate of 0, 100, 325 lb/acre, were selected for detailed sampling and intensive data analysis (see Figure 1). 60 undisturbed soil cores were drilled with a direct-push drilling technique to a depth of 15.8 m (~52 ft).

1.1. Fertilizer Applications

Fertilizer was applied broadcast in September of each year with 100 lbs/acre to all rows except 0 treatment rows and border rows. 175, 250 and 325 subplots received additional fertilizer at the rate of 75 lbs/acre once, twice, and three times, respectively. In the first fertilizer application in September 1982, ammonium sulfate was used. To avoid future soil acidification, ammonium nitrate and calcium nitrate were selected to be used throughout the experiment. For convenience, 100, 0 and 325 lb/acre/year subplots are referred as A, B and C, respectively (e.g., see Figure 9).

1.2. *Core Samples*

On the order of 1,000 samples were taken with locations based on the actual geologic stratification. A complete sedimentologic description by color, texture and moisture was made in the field, and the disturbed samples were further divided for further analysis.

1.2.1. *Soil Hydraulic Properties*

Over 100 undisturbed soil cores were first grouped by sedimentary characteristics and used for multistep outflow experiments to determine unsaturated hydraulic conductivity and soil water retention functions. Prior to this project, the inverse modeling analysis of these experiments were completed to estimate parameters of the constitutive relationships for hydraulic conductivity and water retention curves based on van Genuchten- Mualem model. Summary of basic statistics of the parameters is given in Table 1 for the entire data set, and in Table 2, 3 and 4 for subplot A, B and C respectively. The data for soil hydraulic properties confirms a highly heterogeneous character of the unsaturated zone though the vadose zone. A long tail in the frequency distribution shown in Figure 2a indicates that the data can be expressed by a log normal distribution.

Most of the samples collected were measured for water content θ. The data set shows a wide range of values with an average θ = 0.23 cm^3/cm^3. Analysis of fitting a function to a right-skewed data set indicates that Weibull distribution can better fit the data (Figure 3a). In terms of spatial distribution of the data, all three subplots experience similar trends in the mean θ, increasing with soil depth (Figure 3b).

1.2.2. *Soil Textures*

Several textural units were distinguished in the cores: 1) sand, 2) sandy loam (SL), 3) silt/silt loam/ loam/ silty clay loam (C-Si-L), 4) clay loam/ clay, and 5) hardpan1 (HP1) and hardpan2 (HP2). Sandy loam is the most frequent category within the profile while clay is the least frequent one. Based on the detailed original field description of soil texture data, lithofacies were identified by 7 various units. Figure 4 shows one of the cross sections with lithofacies. A three-dimensional view of lithofacies is also displayed in Figure 4b using the software ArcView. Horizontally connected hardpans, HP1 and HP2, are clearly identified in each core. Interpretation of one of the units was rather difficult due to more than one reoccurring depositional features identified. Therefore, these units were lumped

into *Var* code. *Var* code contains various sedimentary structures within the unit but distinguishable compare to the adjacent facies.

The samples analyzed for soil hydraulic properties were classified by texture by the Division of Agriculture and Natural Resources (DANR) laboratory located at the University of California, Davis. Based on the percentages by weight of sand, silt and clay particles, soil texture was determined through the use of USDA soil textural triangle and shown in Figure 5. Basic statistics of % sand, silt, and clay are given in Table 1 for all data.

1.2.3. Biochemical Properties

Nitrate-N ($NO_3^- - N$) concentration was measured in more than 800 samples with more than 200 samples measured concentration below the detection limit. Additionally, dissolved organic carbon (DOC) and pH were determined. Analysis of ^{15}N isotopes on some of the samples is still ongoing and will be used as an indication of denitrification rates in further analysis. Data analysis indicates highly variable nitrate concentrations throughout the unsaturated zone. In Figure 6a, a frequency distribution of nitrate is shown with a long tail to the right. In Figure 6b, normal distribution is fitted to the log transformed nitrate data. Similarly, frequency distribution of pH, DOC, % soil organic matter and organic carbon are completed. pH data shows a rather acidic to neutral conditions in all three subplots (see Table 1, 2, 3 and 4). The frequency distribution shows that the data is not symmetric, slightly skewed to the left. The representation of pH data by a normal distribution is an approximation that we adopted to use in further analysis. (see Figure 7).

1.3. Irrigation Water Applications

Field averaged water application rates throughout the experiment are obtained for 1983 and 1990-1997 from the records at the Kearney Research Center. The field was flood irrigated. In a typical irrigation approximately 4 in (10 cm) of water are applied with an average application rate of 0.5 cm/hr. An annual average amount of water delivered to the orchard was estimated to be 56 in, which is relatively higher compared to a typical value of 45 in/yr for a well-managed nectarine orchard given under furrow irrigation.

1.4. Precipitation

Climate records from June 1983 to date are obtained from the CIMIS station Parlier (#39), located nearby the research site. Year 1989 was the driest with an averaged annual precipitation of 6.6 while year 1995 was a wet year with the highest annual precipitation of 19.4 in. Reference crop water consumption use (ET_o) provided by CIMIS is used to evaluate evapotranspiration (ET) data for the entire duration of the experiment for known crop coefficients of Kc values.

1.5. Yield and Plant Nutrient Uptake

As part of the fertilizer management project implemented at the site, leaf and fruit nitrogen concentration was analyzed in 1983. Total crop yield was obtained for 7 years during the experiment, from 1983-1985 and 1991-1994. N uptake by plants was available only for 1983. Table 5 shows the yield in kg/acre and the measured N % in dry fruit mass. Yield in 1983 responded positively to the increasing fertilizer rate. 7-year average yield data, however, dropped in all subplots. A significant drop was seen in the control subplot. B subplot must have consumed the reserved N storage at the beginning

of the experiment; thus, there was no significant difference in yield compared to other treatments in 1983. The yield from C gave lower yield than subplot A, indicating a negative response of the system to the high fertilizer application rate.

2. Geostatistical Analysis

Summary of basic statistics of all data is represented in Table 1. Tables 2, 3 and 4 show the statistics categorized by subplots. Using available geostatistical software (Tecplot), kriging is used to interpolate the point samples of nitrate, pH and water content into a continuous three-dimensional domain. The spatial distribution of pH predicted by kriging is shown in Figure 8a. Since nitrate is measured on a dry soil basis, proper estimation of water content is critical to estimating nitrate mass. Water content distribution at each subplot is presented in Figure 8b. Two sets of evaluations are performed on the log transformed nitrate data: 1) based on N concentration defined on a dry soil mass (ug N/g dry soil, Figure 9a), and 2) as a solution concentration (ug N/mL water, Figure 9b).

Semivariograms are computed as part of the above geostatistical analysis to investigate spatial continuity of nitrate data. Semi-variograms were computed in the horizontal and vertical directions. Three-dimensionally uni-directional variograms were also computed (variograms that ignore any directional influence in spatial continuity). Uni-directional variograms show a fairly clear structure with a range of approximately 20 ft, as shown in Figure 10a, 11a and 12a in subplot A, B and C respectively. Large fluctuations beyond the lag distance of 20 ft may suggest that observation pairs that are far enough a part in the horizontal direction are dissimilar. Variograms in the vertical directions indicate a significantly larger continuity (larger range), smaller sills and relatively small fluctuations. A spherical model is fit to the experimental data. The model fitting parameters, nugget, sill and range are listed in Table 6. An overlay of the model semivariogram is also displayed in Figure 10 through 12. The horizontal variogram reveals that spatial continuity in the horizontal direction is much shorter (10 ft. to 15 ft.) than in the vertical direction (28 ft. – 35 ft.). The horizontal variogram data fluctuate significantly more due to the larger sample spacing in the horizontal direction and the lower number of sampling pairs for the variogram analysis; thus, the spherical model variogram is only a rough approximation.

3. Nitrate Budget

Three alternative N management practices with an annual fertilizer rate of 0, 100 and 325 lbs N/ac are compared to estimate the risk of nitrate loss from the root zone. Two methods are employed to estimate field scale N budget. The first method includes approximate quantification of annual N fluxes due to dominant processes and examining the corresponding annual balance of N. To accomplish our goal, dominant N cycle processes are identified from field trial data and literature reference values, where needed. In the second method, kriging interpolation is used to estimate nitrate mass distribution at the three management sites based on 800 samples collected in 60 boreholes to 15 m depth. Analysis is performed on both N concentration defined on a dry soil mass (ug N/g dry soil) and as a solution concentration (ug N/mL water). The results from both of the latter two analyses are consistent. The final nitrogen mass is interpreted as excess N potentially susceptible to leaching. The N budget determined using the kriging approach resulted in significantly less excess N found in the system than the

mass balance method predicted. This result indicates that other processes (denitrification, dilution) must be identified to explain the loss of mass. This phase of the project emphasizes the significance of field measurements for addressing uncertainty in predictions of leachable nitrate to groundwater. Results from this study can be used as an indication of environmental impact of agricultural production on water quality.

Table 1. Basic statistics of the data from all three subplots A, B and C.

Data	# of data	Mean	Confidence -95%	Confidence 95 %	Median	Minimum	Maximum	Lower Quartile	Upper Quartile	Variance	Standard Deviation	Skewness
θ (cm^3/cm^3)	1183	0.23	0.22	0.24	0.21	0.00	0.59	0.13	0.32	0.02	0.12	0.50
pH	935	7.03	7.01	7.05	7.07	5.35	7.82	6.85	7.26	0.12	0.34	-0.95
ln NO3 (ug/mL)	585	0.80	0.70	0.90	0.94	-3.24	4.87	0.18	1.50	1.54	1.24	-0.46
Bulk density (g/cm3)	119	1.62	1.60	1.64	1.60	1.26	1.87	1.52	1.74	0.02	0.13	-0.07
% OM	119	0.09	0.09	0.10	0.09	0.01	0.20	0.07	0.12	0.00	0.04	0.46
% Org-C	95	0.05	0.05	0.06	0.05	0.01	0.12	0.04	0.07	0.00	0.02	0.75
% Sand	119	69.54	65.63	73.45	72.00	13.00	99.00	61.00	83.00	464.23	21.55	-0.79
% Silt	119	25.26	21.58	28.94	21.00	0.10	81.00	14.00	32.00	410.95	20.27	0.98
% Clay	119	5.26	4.64	5.89	4.00	0.10	17.00	3.00	7.00	11.92	3.45	0.84
K (measured) (cm/hr)	109	12.73	7.24	18.23	0.66	0.00	100.00	0.19	4.27	837.94	28.95	2.45
□ (1/cm)	97	0.03	0.00	0.06	0.01	0.00	1.48	0.01	0.02	0.02	0.15	9.67
n	97	2.61	2.34	2.89	2.36	0.00	7.47	1.66	3.14	1.84	1.36	1.30
Residual θ (cm^3/cm^3)	97	0.11	0.10	0.13	0.09	0.00	0.40	0.05	0.15	0.01	0.09	1.03
Saturated θ (cm^3/cm^3)	118	0.31	0.30	0.32	0.30	0.13	0.47	0.26	0.34	0.00	0.06	0.49
DOC (ppm)	449	1.76	1.72	1.81	1.73	0.23	3.19	1.62	1.95	0.20	0.45	-0.39

Table 2. Basic statistics of the data in subplot A, 100 lbs N/ac/yr treatment.

Data	# of data	Mean	Confidence -95%	Confidence 95 %	Median	Minimum	Maximum	Lower Quartile	Upper Quartile	Variance	Standard Deviation	Skewness
θ (cm^3/cm^3)	391	0.23	0.22	0.25	0.22	0.01	0.54	0.15	0.32	0.01	0.12	0.46
pH	281	6.96	6.91	7.01	7.03	5.35	7.80	6.75	7.24	0.18	0.43	-0.83
ln NO3 (ug/mL)	277	0.59	0.46	0.72	0.77	-2.63	4.34	0.08	1.22	1.22	1.11	-0.67
Bulk density (g/cm3)	47	1.61	1.57	1.65	1.58	1.31	1.87	1.49	1.74	0.02	0.14	0.20
% OM	47	0.10	0.08	0.11	0.09	0.01	0.20	0.07	0.13	0.00	0.04	0.45
% Org-C	29	0.05	0.04	0.06	0.05	0.01	0.12	0.04	0.06	0.00	0.03	0.82
% Sand	47	69.38	62.91	75.86	72.00	13.00	99.00	57.00	83.00	486.63	22.06	-0.87
% Silt	47	25.92	19.97	31.88	23.00	0.10	81.00	13.00	35.00	411.28	20.28	0.96
% Clay	47	4.73	3.71	5.74	4.00	0.10	17.00	3.00	7.00	11.99	3.46	1.49
K (measured) (cm/hr)	37	26.09	11.66	40.52	0.66	0.00	100.00	0.19	51.15	1873.54	43.28	1.16
□ (1/cm)	26	0.01	0.01	0.02	0.01	0.00	0.05	0.00	0.02	0.00	0.01	1.64
n	26	2.88	2.17	3.59	2.32	1.21	7.47	1.67	3.14	3.12	1.77	1.52
Residual θ (cm^3/cm^3)	26	0.11	0.07	0.15	0.08	0.00	0.36	0.03	0.17	0.01	0.10	0.91
Saturatedθ (cm^3/cm^3)	46	0.31	0.30	0.33	0.31	0.22	0.43	0.26	0.34	0.00	0.05	0.35
DOC (ppm)	235	1.84	1.80	1.87	1.77	1.11	2.94	1.64	2.01	0.08	0.29	1.10

Table 3. Basic statistics of the data in subplot B, the control subplot.

Data	# of data	Mean	Confidence -95%	Confidence 95 %	Median	Minimum	Maximum	Lower Quartile	Upper Quartile	Variance	Standard Deviation	Skewness
θ (cm^3/cm^3)	378	0.23	0.21	0.24	0.20	0.00	0.57	0.13	0.31	0.02	0.12	0.53
pH	340	7.10	7.08	7.13	7.09	6.51	7.62	6.97	7.28	0.05	0.22	-0.07
ln NO3 (ug/mL)	158	0.69	0.47	0.90	0.85	-2.78	4.65	-0.23	1.55	1.91	1.38	-0.25
Bulk density (g/cm3)	37	1.63	1.59	1.66	1.63	1.32	1.87	1.55	1.71	0.01	0.11	-0.27
% OM	37	0.09	0.08	0.11	0.09	0.01	0.20	0.07	0.12	0.00	0.04	0.39
% Org-C	32	0.05	0.05	0.06	0.05	0.02	0.12	0.04	0.07	0.00	0.02	0.84
% Sand	37	71.30	64.46	78.13	74.00	15.00	99.00	66.00	83.00	420.38	20.50	-1.16
% Silt	37	22.71	16.33	29.09	20.00	0.10	76.00	15.00	24.00	366.17	19.14	1.45
% Clay	37	6.03	4.81	7.25	6.00	0.10	13.00	4.00	9.00	13.38	3.66	0.16
K (measured) (cm/hr)	37	3.83	1.41	6.25	0.81	0.00	33.90	0.19	4.20	52.62	7.25	2.98
□ (1/cm)	36	0.02	0.01	0.03	0.01	0.00	0.08	0.01	0.02	0.00	0.02	1.84
n	36	2.60	2.19	3.01	2.53	1.12	5.30	1.59	3.44	1.44	1.20	0.67
Residual θ (cm^3/cm^3)	36	0.12	0.09	0.15	0.09	0.00	0.40	0.07	0.16	0.01	0.09	1.50
Saturated θ	37	0.30	0.28	0.32	0.28	0.13	0.44	0.26	0.33	0.00	0.06	0.30

(cm^3/cm^3)												
DOC (ppm)	140	1.67	1.57	1.76	1.69	0.23	3.19	1.51	1.81	0.33	0.57	-0.14

Table 4. Basic statistics of the data in subplot C, 325 lbs N/ac/yr treatment.

Data	# of data	Mean	Confidence -95%	Confidence 95 %	Median	Minimum	Maximum	Lower Quartile	Upper Quartile	Variance	Standard Deviation	Skewness
θ (cm^3/cm^3)	310	0.23	0.21	0.24	0.21	0.01	0.59	0.13	0.33	0.02	0.13	0.50
pH	314	7.02	6.98	7.06	7.07	5.83	7.82	6.79	7.27	0.12	0.35	-0.62
ln NO3 (ug/mL)	150	1.30	1.11	1.49	1.41	-3.24	4.87	0.76	1.95	1.41	1.19	-0.74
Bulk density (g/cm3)	35	1.63	1.57	1.68	1.62	1.26	1.87	1.51	1.77	0.02	0.15	-0.26
% OM	35	0.09	0.08	0.10	0.08	0.04	0.17	0.06	0.12	0.00	0.04	0.52
% Org-C	34	0.05	0.04	0.06	0.05	0.02	0.10	0.03	0.07	0.00	0.02	0.54
% Sand	35	67.89	60.19	75.58	70.00	25.00	99.00	49.00	87.00	501.46	22.39	-0.42
% Silt	35	27.07	19.62	34.53	21.00	0.10	71.00	15.00	44.00	471.03	21.70	0.69
% Clay	35	5.17	4.09	6.26	5.00	0.10	15.00	3.00	7.00	9.94	3.15	0.87

K (measured) (cm/hr)	35	8.02	1.88	14.15	0.64	0.01	72.47	0.20	5.25	318.98	17.86	2.81
□ (1/cm)	35	0.06	-0.03	0.14	0.01	0.00	1.48	0.00	0.01	0.06	0.25	5.88
n	35	2.43	2.04	2.83	2.15	0.00	5.24	1.55	3.06	1.34	1.16	0.75
Residual θ (cm^3/cm^3)	35	0.11	0.08	0.14	0.09	0.00	0.34	0.04	0.15	0.01	0.09	0.85
Saturatedθ (cm^3/cm^3)	35	0.31	0.29	0.33	0.30	0.23	0.47	0.27	0.35	0.00	0.06	0.92
DOC (ppm)	74	1.71	1.57	1.84	1.75	0.25	2.72	1.40	1.96	0.34	0.58	-0.40

Table 5. Yield data and N % measured based on dry fruit mass for 1983. Average yield is obtained from the data of 1983-1985 and 1991-1994.

subplot N lbs/N/ac/yr	1983 yield ton/acre	N %	7 year avg. yield ton/acre
0	20.82	0.71	14.56
100	22.06	1.51	20.66
175	21.68	1.66	19.84
250	21.95	1.78	21.23
325	22.18	2.05	19.37

Table 6. Parameters of the model variograms fitted to the experimental variograms in three directions in subplot A, B and C.

subplot	direction	model type	nugget	sill	range
A	uni-direction	spherical	1.3	5.25	12
	horizontal		1.1	6	10
	vertical		1.8	4.2	34.25
B	uni-direction	spherical	0.8	4.7	7.3
	horizontal		2.7	2.1	13
	vertical		3.5	3.14	34
C	uni-direction	spherical	1.4	5.8	12
	horizontal		1.5	6.55	14.5
	vertical		2.7	5	28

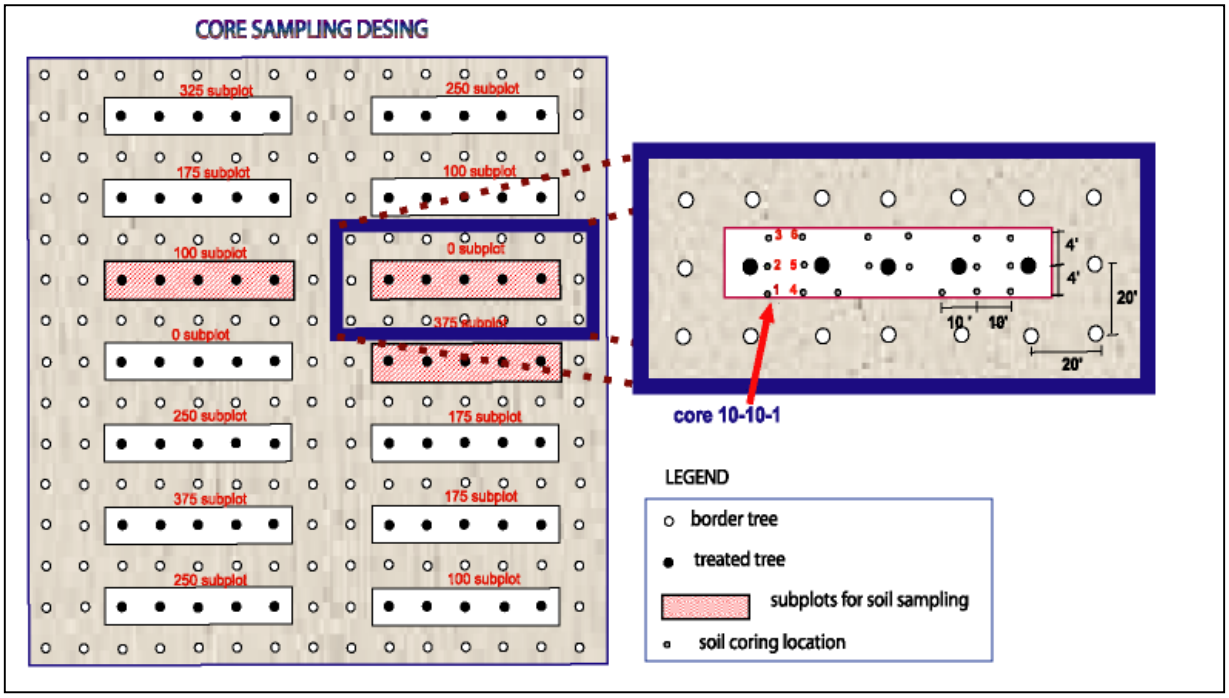

Figure 1. Field experiment design showing the locations of the cores.

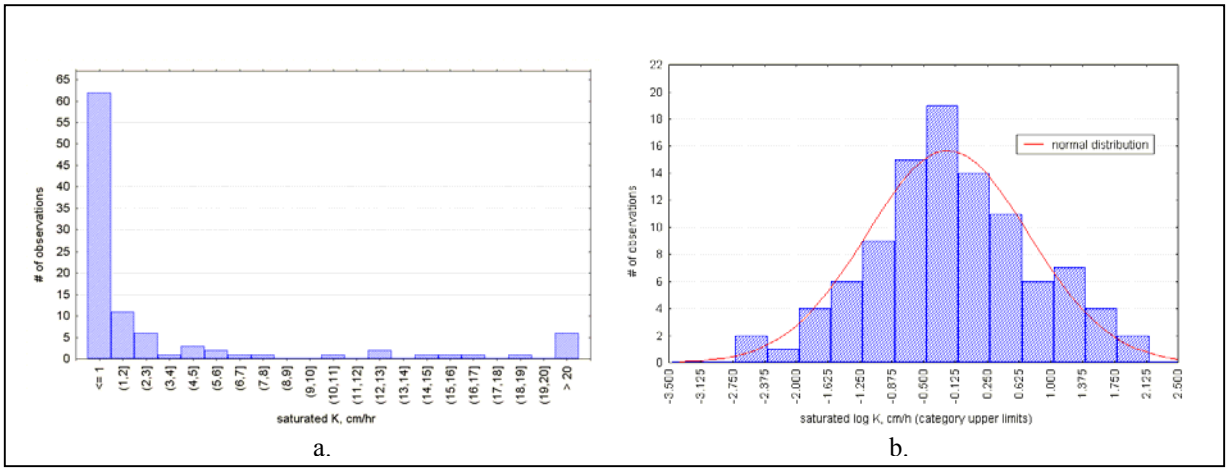

a. b.

Figure 2. Distribution of saturated hydraulic conductivity, a) frequency distribution, b) saturated K fitted to a log normal distribution.

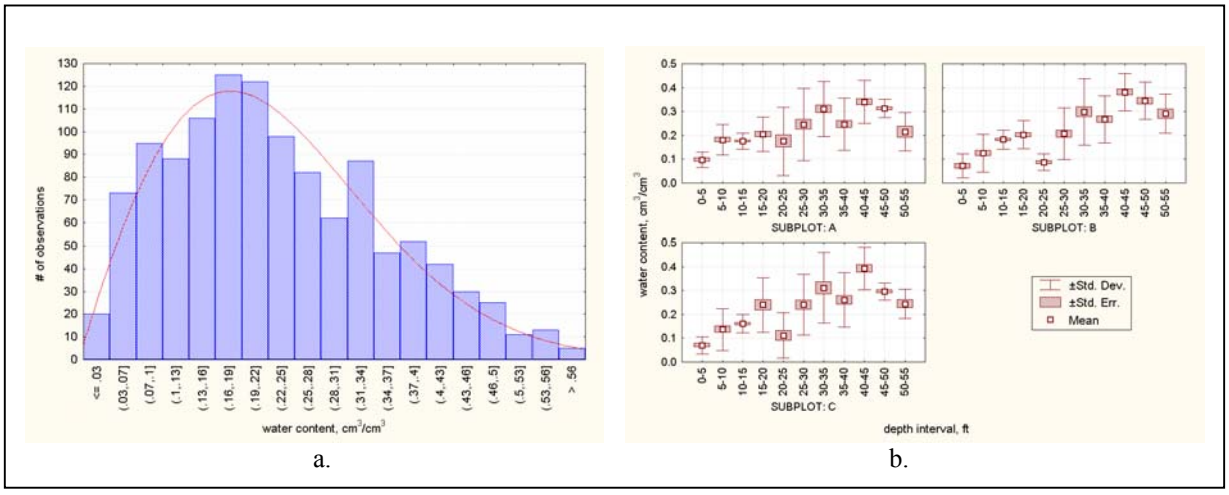

a. b.

Figure 3. Distribution of water content, a) frequency distribution fitted to two-parameter Weibull distribution, b) box and whisker plot of mean water content throughout the soil profile.

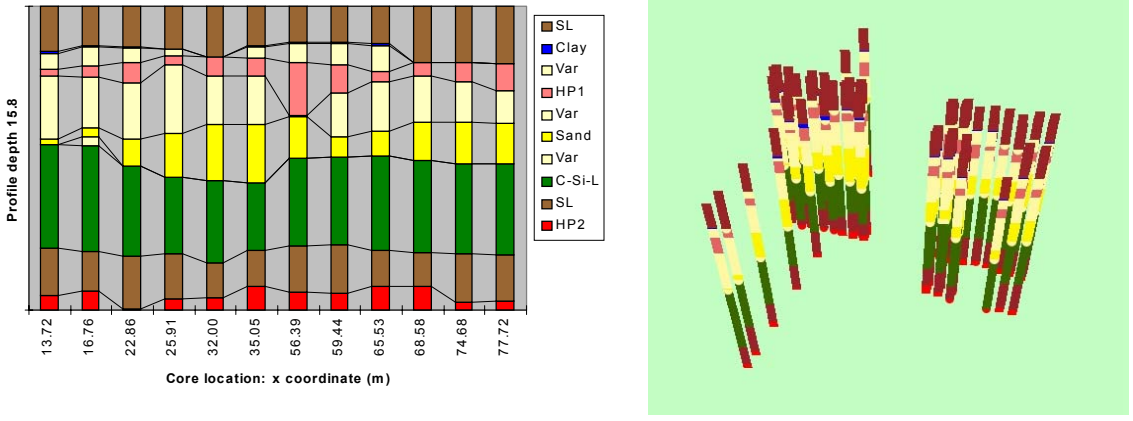

a. b.

Figure 4. a) lithofacies created from soil texture data from east to west at y = 54.08 m, b) display of lithofacies in three dimensions.

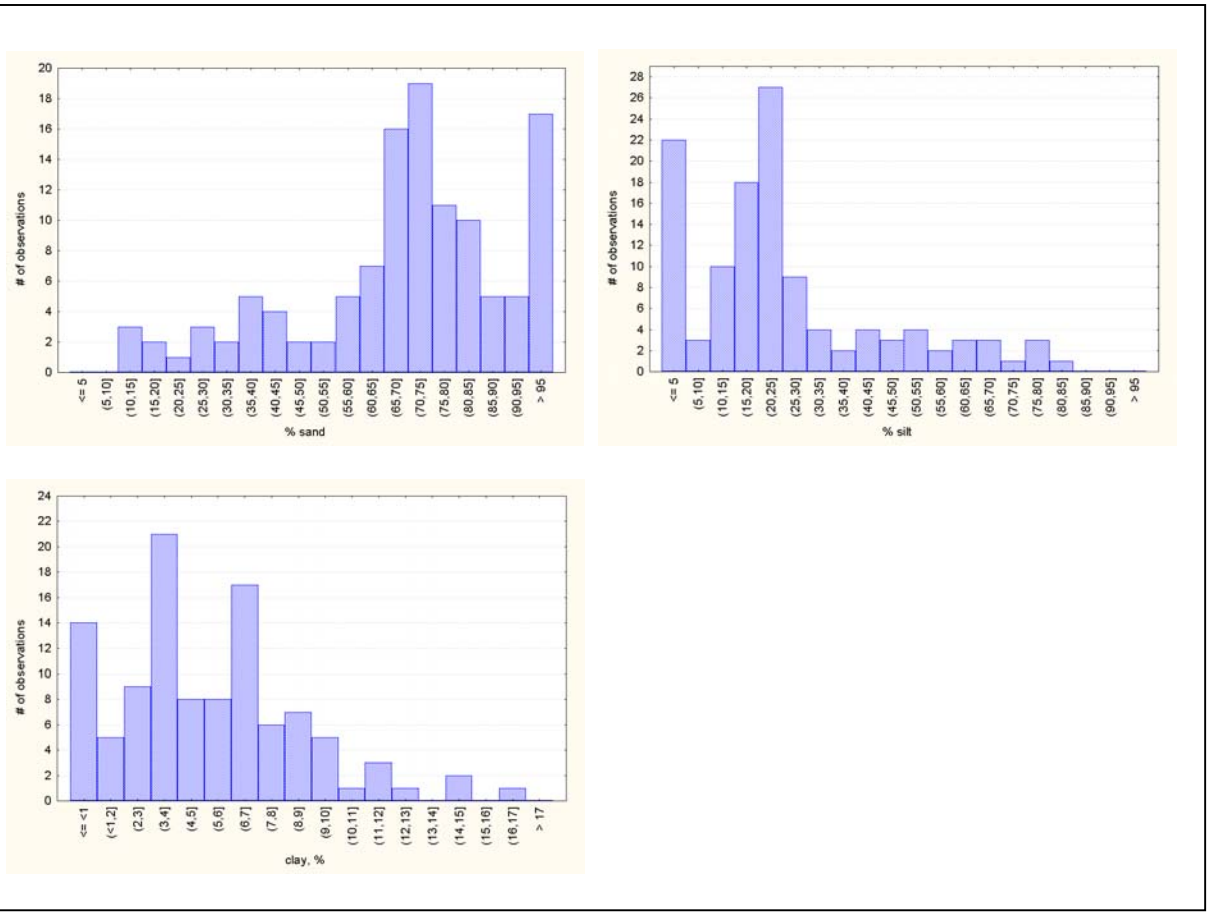

Figure 5. Distribution of sand, silt and clay percentages.

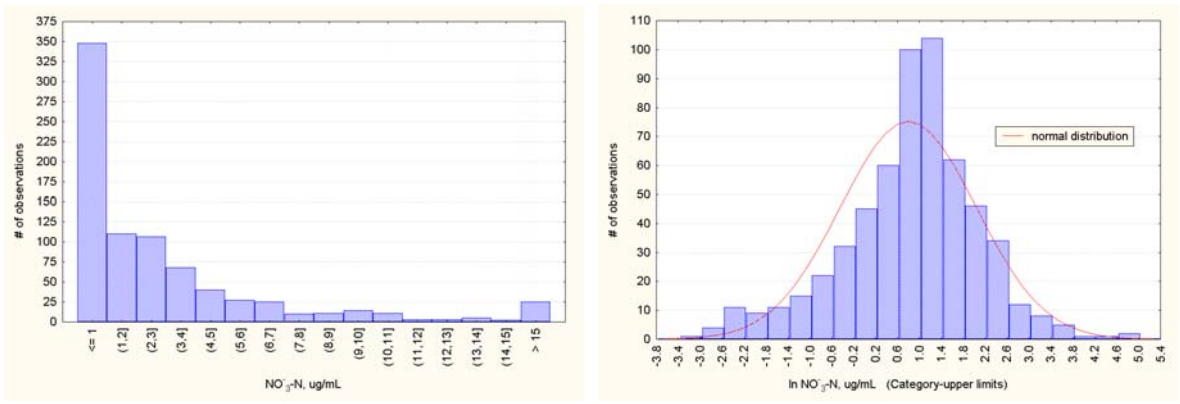

a. b.

Figure 6. a) Frequency distribution of nitrate, b) log transformed data fitted to normal distribution.

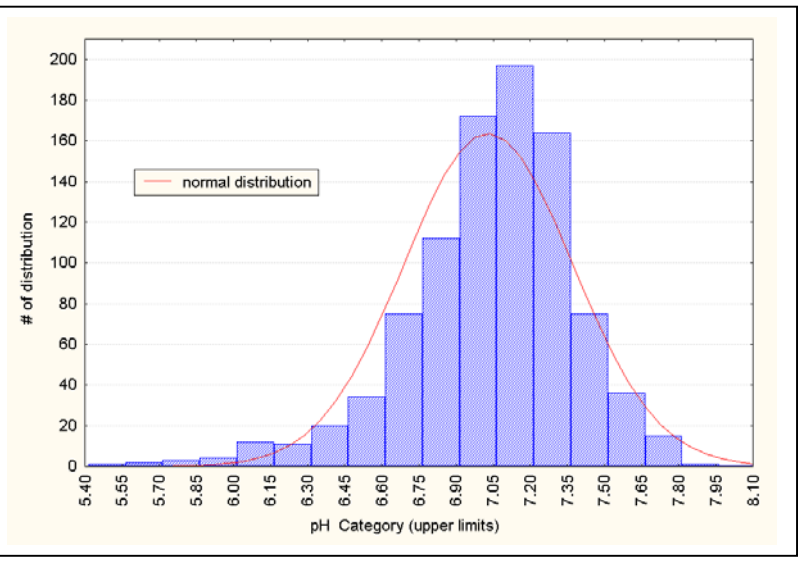

Figure 7. Frequency distribution of pH fitted to normal distribution, b) frequency distribution of pH.

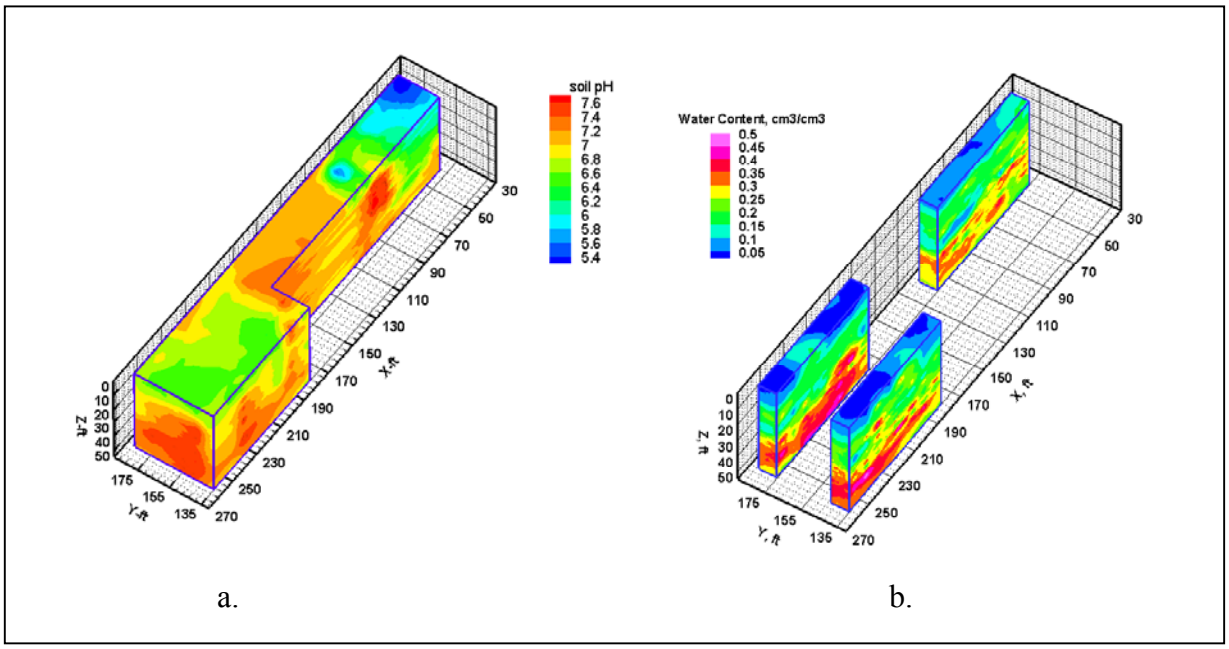

Figure 8. a) A three dimensional spatial distribution of pH and b) water content at each subplot.

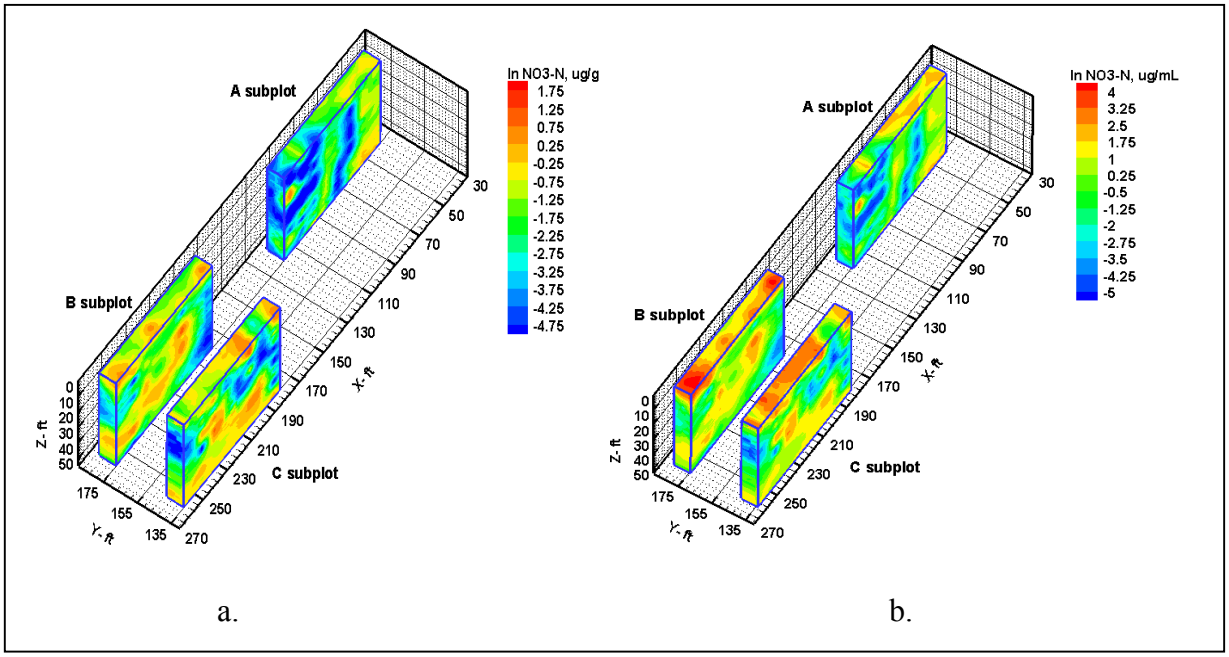

Figure 9. a) A three dimensional spatial distribution of nitrate at each subplot a) based on N concentration defined on a dry soil mass (ug N/g dry soil), and b) as a solution concentration (ug N/mL water).

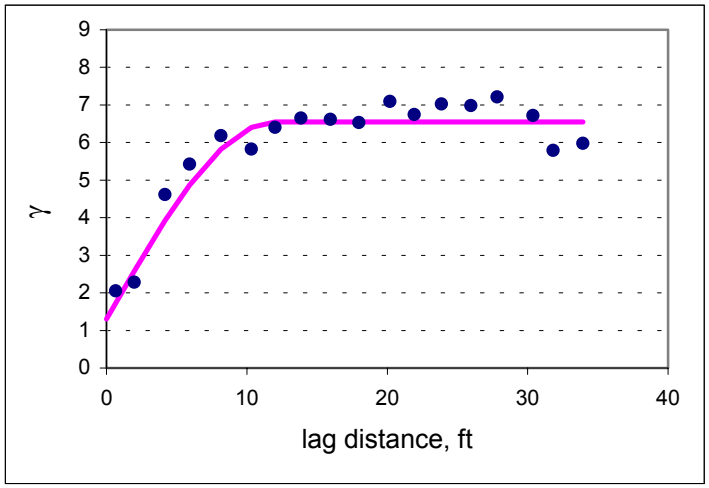

a)

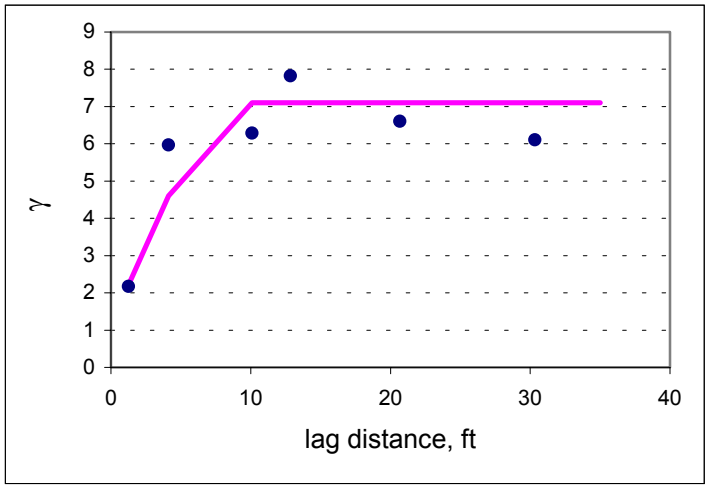

b)

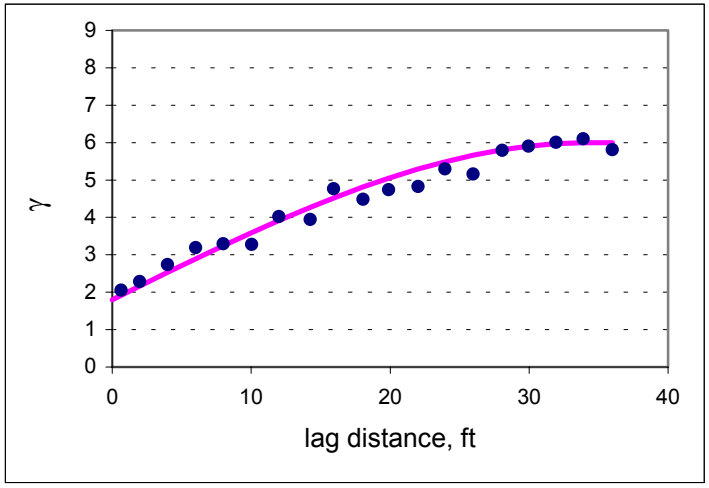

c)

Figure 10. Comparision of experimental semivariogram with semivariogram models for NO3 data in subplot A. Dots denote experimental values and lines denote spherical semivariogram models. Experimental and spherical model semivariogram a) in the uni-direction, b) in the horizontal direction and c) in the vertical direction.

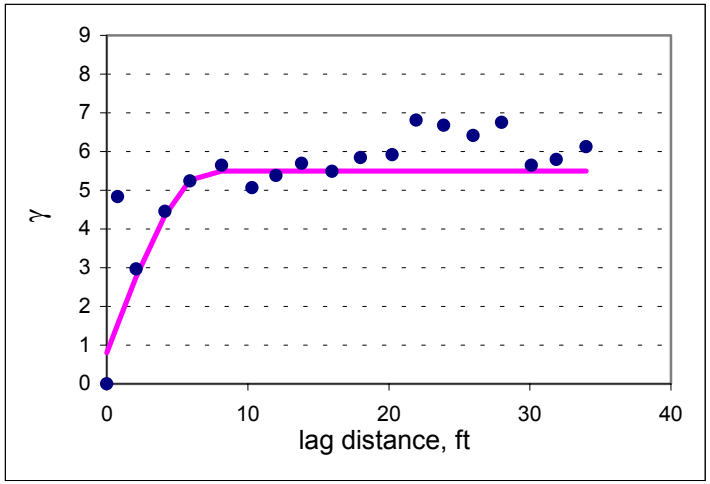

a)

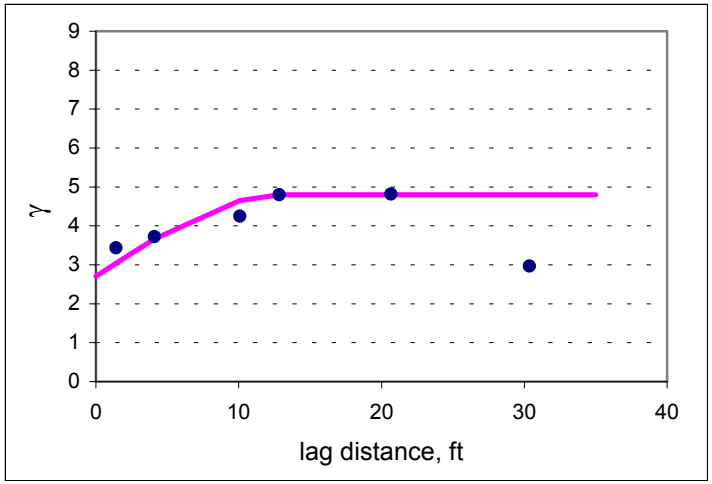

b)

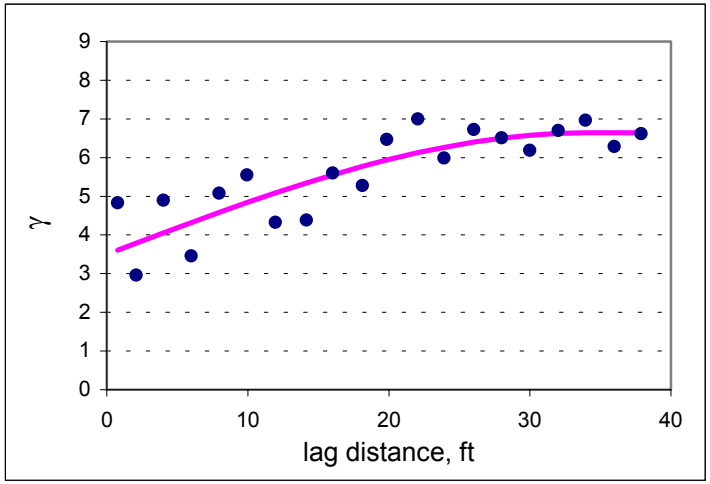

c)

Figure 11. Comparision of experimental semivariogram with semivariogram models for NO3 data in subplot B. Dots denote experimental values and lines denote spherical semivariogram models. Experimental and spherical model semivariogram a) in the uni-direction, b) in the horizontal direction and c) in the vertical direction.

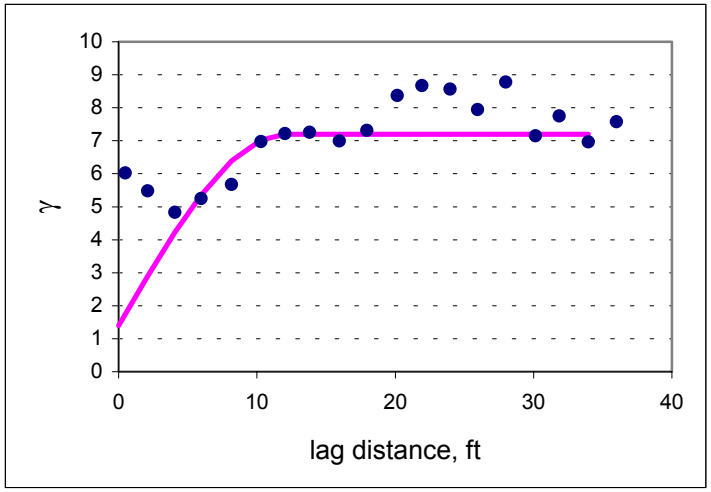

a)

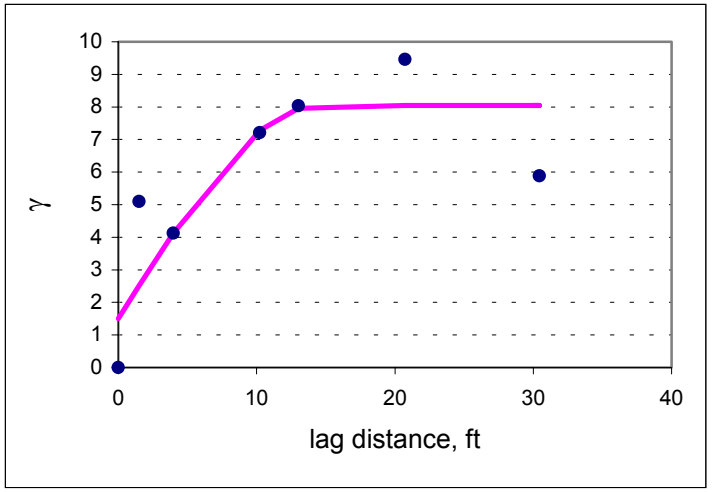

b)

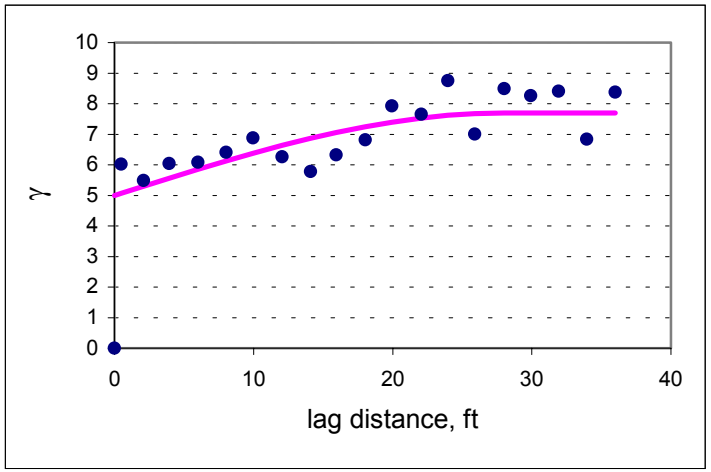

c)

Figure 12. Comparision of experimental semivariogram with semivariogram models for NO3 data in subplot C. Dots denote experimental values and lines denote spherical semivariogram models. Experimental and spherical model semivariogram a) in the uni-direction, b) in the horizontal direction and c) in the vertical direction.